

Article

Structural Properties of a Heteropolysaccharide Released from *Isaria cicadae* Miq. Solid-State Fermented Wheat Bran

Rui Liu ¹, Ruixin Liu ¹, Xuebing Yan ¹, Ningjie Li ^{1,2}, Ming Li ³, Zijian Zhi ⁴, Boli Guo ^{3,*} and Min Zhang ^{1,*}

¹ State Key Laboratory of Food Nutrition and Safety, Tianjin University of Science & Technology, Tianjin 300457, China

² Key Laboratory of Natural Products, Henan Academy of Sciences, Zhengzhou 450002, China

³ Institute of Food Science and Technology CAAS, Beijing 100193, China

⁴ Food Structure and Function (FSF) Research Group, Department of Food Technology, Safety and Health, Faculty of Bioscience Engineering, Ghent University, Coupure Links 653, 9000 Gent, Belgium

* Correspondence: guoboli@caas.cn (B.G.); zm0102@sina.com (M.Z.)

Abstract: The work aimed to improve the extraction efficiency of wheat bran polysaccharide by solid-state fermentation using the bioactive fungus *Isaria cicadae* Miq. and identify the structural properties of fermented wheat bran polysaccharide (IC-FWBP). The polysaccharide fraction of IC-FWBP was isolated with an extraction yield of 2.88% and an average molecular weight of 3.31×10^6 Da. The IC-FWBP was comprised of mannose, glucose, and galactose. The methylation, nuclear magnetic resonance (NMR), and Congo red analysis results suggested that IC-FWBP contained glycosidic linkages of T- β -D-Glcf, 1 \rightarrow 2- α -D-Manp, 1 \rightarrow 5,6- β -D-Galf, 1 \rightarrow 2,3,4- α -D-Galp and 1 \rightarrow 2,3,4- β -D-Manp, with triple-helix conformations. The morphological observation showed that IC-FWBP was composed of rod-like and spherical particles. These investigations on the structural properties of IC-FWBP will be beneficial to further research on the functional properties of wheat bran polysaccharides.

Keywords: solid-state fermentation; wheat bran; Cordyceps fungi; polysaccharides; structural properties



Citation: Liu, R.; Liu, R.; Yan, X.; Li, N.; Li, M.; Zhi, Z.; Guo, B.; Zhang, M. Structural Properties of a Heteropolysaccharide Released from *Isaria cicadae* Miq. Solid-State Fermented Wheat Bran. *Fermentation* **2023**, *9*, 309. <https://doi.org/10.3390/fermentation9030309>

Academic Editor: Yuxia Mei

Received: 24 February 2023

Revised: 17 March 2023

Accepted: 20 March 2023

Published: 21 March 2023



Copyright: © 2023 by the authors. Licensee MDPI, Basel, Switzerland. This article is an open access article distributed under the terms and conditions of the Creative Commons Attribution (CC BY) license (<https://creativecommons.org/licenses/by/4.0/>).

1. Introduction

As a naturally complex macromolecular compound, polysaccharides are a class of carbohydrates whose molecules are made up of various polymeric monosaccharide units in a linear or branched chain [1]. They are widely found in plants, animals, microorganisms and marine life [2]. Natural polysaccharides have attracted much attention for their multiple functions, including antioxidant, antitumor, immunomodulatory, hypoglycemic, antithrombotic and anticoagulant activities [3–5]. These functional properties of polysaccharides are profoundly associated with their chemical structural features, for instance, monosaccharide composition, molecular weight and chemical structure [6,7]. Understanding the chemical structure of polysaccharides from more sources can be of great help in studying the structure-activity relationship of polysaccharides.

Wheat bran is an available and abundant by-product of the wheat flour processing industry, typically comprising 14%–19% of the total weight of grain wheat [8]. Wheat bran is rich in dietary fiber, of which arabinoxylan (AX) is the main component, accounting for nearly 70% of the total [9]. The application of microorganisms in the high-value utilization of wheat bran has been extensively studied. In the fermentation process, the active components of raw materials can be decomposed to produce new active substances through microbial growth and metabolism [10]. Chen et al. [11] used *Saccharomyces cerevisiae* and *Bacillus subtilis* to ferment wheat bran, and the results showed that fermentation could change the structural characteristics of wheat bran polysaccharides and improve their antioxidant activity. The results of [12] show that *Eurotium cristatum* produced β -hydroxy acid metabolites of monacolin K and improved bioactive compound contents as well as functional properties in fermented wheat bran.

Isaria cicadae Miq. (IC) is a kind of Cordyceps fungus, and its polysaccharide has a strong effect on enhancing immune function [13]. IC is widely used as a tonic for nourishment as well as a functional food that possesses remarkable biological activity, including immunomodulatory activity, antioxidation, anti-aging, antitumor, antiinflammation and amelioration of renal function [14,15]. Xu et al. [13] isolated and purified two heteropolysaccharides from IC with different immunomodulatory activities, which were composed of mannose, glucose and galactose with different ratios. Herein, the purpose of applying IC to solid-state fermentation (SSF) of wheat bran was to increase the ratio of functional polysaccharide in IC solid-state fermented wheat bran substrates and to further explore the structural characteristics of polysaccharide components from the fermented wheat bran.

In this study, heteropolysaccharide was isolated and purified from solid-state fermented wheat bran by IC strains to identify the chemical composition and structural features of IC-fermented wheat bran polysaccharide (IC-FWBP). Furthermore, the conformation, morphology and thermal stability of the IC-FWBP were examined by Congo red analysis, scanning electron microscopy (SEM), atomic force microscopy (AFM), thermogravimetric analysis (TGA) and differential scanning calorimetry (DSC). These investigations on polysaccharide structure will be beneficial to further research on the relationship between structure and biological activity of the FWBP from IC solid-state fermented wheat bran.

2. Materials and Methods

2.1. Materials

Wheat bran was kindly provided by Fada Flour Company (Shandong Province, China) and was finely ground to pass through a 0.45 mm mesh screen. The chemical composition of the wheat bran powder is given in Table S1. *Isaria cicadae* Miq. (IC) was purchased from Beijing Beina Chuanglian Biotechnology Research Institute, China. All standard chemicals and reagents used were of analytical grade.

2.2. Sample Preparation

The moisture content of the wheat bran was adjusted to 50% before sterilization. The fermented wheat bran was prepared by inoculating 5 g of sterilized wheat bran with pre-cultured IC strains (10% on a basis of dry wheat bran) at 27 °C, and the solid-state fermentation (SSF) process was maintained for 6 days. The fermented wheat bran was then dried at 45 °C for 48 h and then ground into a fine powder with a universal high-speed smashing machine for further use.

2.3. Extraction and Purification of Polysaccharides from Wheat Bran

The extraction of polysaccharides mostly adopts the method of water extraction and alcohol precipitation. Polysaccharides are soluble in water, and the addition of ethanol will destroy the hydrogen bonding of the polysaccharide in an aqueous solution, thus making the polysaccharide precipitate. The principle of polysaccharide separation in the DEAE cellulose anionic column is that it can adsorb ionic substances, thus separating acidic and neutral sugars, and the best elution mode was found by using linear gradient elution [16]. The specific operation method is as follows:

The unfermented and IC-fermented wheat bran powder was extracted with distilled water (1:20, *w/v*) at 85 °C for 2 h with constant stirring. The supernatant was collected by centrifugation at 4000 r/min for 10 min and then concentrated on a rotary evaporator at 50 °C under reduced pressure. The concentrate was precipitated with four volumes of 95% (*v/v*) ethanol at 4 °C overnight. After centrifugation at 4000 r/min for 20 min, the precipitate was dissolved in distilled water. Then, protein was removed by the Sevage method four times, followed by concentration to one-tenth of the original volume under vacuum. After lyophilization, raw wheat bran polysaccharides (RWBPs) and crude IC-fermented wheat bran polysaccharides were obtained.

The medium pressure column was selected for column loading, which was continuously balanced for 12 h with distilled water. A portion of the crude polysaccharide sample (20 mg/mL) was loaded onto a pre-equilibrated cellulose DEAE-52 column (1.6 cm × 300 cm) and sequentially eluted with distilled water and 0.1, 0.2, 0.4 and 0.6 M sodium chloride solutions at a flow rate of 1.0 mL/min. The automatic collector collects 5 mL for each tube and 24 tubes for each concentration. The polysaccharide content of each tube was analyzed using the phenol-sulfuric acid method at 490 nm [17]. The polysaccharide solution was dialyzed against a dialysis bag (Genview, Tallahassee, Florida, USA) of 100 kDa for 48 h to remove small molecule impurities and then freeze-dried for 48 h to collect the IC-FWBP fraction.

2.4. Chemical Composition Analysis

The chemical composition, including carbohydrate, protein and uronic acid contents, was analyzed. Carbohydrate content was determined by the phenol-sulfuric acid method [17]. Protein content was determined by the Coomassie brilliant blue method [18]. Uronic acid content was analyzed using the sulfuric acid-carbazole method [19].

2.5. Molecular Weight Determination

The homogeneity and molecular weight of IC-FWBP were determined by size-exclusion chromatography (SEC) on a high-performance liquid chromatography system (LC-20AT, Shimadzu, Japan) equipped with a refractive index detector (RID-10A, Shimadzu, Japan) and a Shodex OHpak SB-805 HQ column (8.0 mm × 300 mm), eluted by ultrapure water at a flow rate of 1.0 mL/min and maintained at 30 °C. A 20 µL sample (1.0 mg/mL) was injected in each run. The average molecular weight (M_w) of the IC-FWBP was calculated using the calibration curve of dextran standards (Sigma-Aldrich, Shanghai, China), with M_w of 5300, 3755, 2400, 2000, 500, 110, 70, and 40 kDa.

2.6. Monosaccharide Composition Analysis

Monosaccharide compositions of IC-FWBP were analyzed by gas chromatography-mass spectrometry (GC-MS). Briefly, a portion of the IC-FWBP (10 mg) was hydrolyzed with 1 mL of 2 M trifluoroacetic acid (TFA) into monosaccharides at 120 °C for 4 h. The released monosaccharides were completely reduced by using 30 mg sodium borohydride (NaBH_4) in 2 mL distilled water at room temperature for 1.5 h, followed by neutralization with glacial acetic acid to remove the excess NaBH_4 . The mixture was treated with methanol hydrochloride solution (0.1%, *v/v*) four times and then dried at 105 °C for 15 min. The alditol acetate derivatives of monosaccharides were produced by acetylation using 1 mL pyridine/acetic anhydride (1:1, *v/v*) at 105 °C for 1 h. The acetylated products were analyzed on a Shimadzu GC-MS QP2010 Ultra system fitted with an Rtx-5MS capillary column (30 m × 0.32 mm × 0.25 µm). The operation conditions were as follows: injection volume, 0.2 µL; He (1.0 mL/min); injection temperature, 280 °C; column temperature programmed from 100 °C to 260 °C at 10 °C/min; 260 °C for 5 min.

2.7. Periodate Oxidation and Smith Degradation Analysis

Periodate oxidation was performed according to the method described in a previous report [20], with slight modifications. Briefly, the IC-FWBP (10 mg) was dissolved in a 30 mM sodium periodate (NaIO_4) solution, made up to 20 mL and incubated at 4 °C in the darkness. When the reaction was stable, the solution (2 mL) was mixed with 0.2 mL of ethylene glycol to terminate the reaction. The resulting formic acid was titrated with a 0.01 M sodium hydroxide (NaOH) solution. The residual solution was dialyzed (M_w cut-off = 3500 Da) against distilled water for 48 h for Smith degradation.

Smith degradation was performed as described in a previous report [21], with slight modifications. Briefly, the above IC-FWBP solution was reduced with 30 mg of NaBH_4 at 4 °C for 12 h in darkness and neutralized to pH 5.5 with glacial acetic acid. The lyophilized sample (10 mg) was hydrolyzed using 1 mL of TFA (2 M) at 120 °C for 6 h. The product was

acetylated as described in 2.6, and then all the derivatives were analyzed by GC (Agilent 7890A, Palo Alto, CA, USA).

2.8. Methylation Analysis

The IC-FWBP sample was methylated according to previous reports [22]. A portion of the IC-FWBP (10 mg) and NaOH powder (50 mg) were dissolved in 2 mL of anhydrous dimethyl sulfoxide (DMSO) under a nitrogen atmosphere, mixed with 1 mL of methyl iodide (CH₃I) and sonicated in the darkness at 20 °C for 1 h. The reaction was terminated by adding 0.5 mL of distilled water. The methylated IC-FWBP was extracted with an equal volume of dichloromethane (CH₂Cl₂) three times, and the total extracts were evaporated to dryness. This process was repeated eight times until the IC-FWBP was completely methylated. The dried methylated IC-FWBP sample was then hydrolyzed, reduced and acetylated as previously described. The final analyte was injected into the Scion TQ GC-MS (Bruker Daltonics Inc., Santa Barbara, CA, USA), and its relative molar ratio was calculated using the peak area normalization method.

2.9. Nuclear Magnetic Resonance Analysis

IC-FWBP (30 mg) was dissolved in 0.6 mL of D₂O (99.9%) and then added into an NMR sample tube [23]. ¹H nuclear magnetic resonance (¹H NMR), ¹³C nuclear magnetic resonance (¹³C NMR), ¹H-¹H correlation spectroscopy (¹H-¹H COSY), heteronuclear single quantum coherence (HSQC), and heteronuclear multiple bond correlation (HMBC) spectra were recorded on a Bruker Avance III 400 MHz NMR spectrometer (Cambridge Isotope Laboratories, Inc., MA, Boston, USA).

2.10. Fourier-Transform Infrared Spectral Analysis

The dried IC-FWBP (1 mg) was ground with 100 mg of potassium bromide and then pressed into a pellet for Fourier transform infrared (FTIR) spectral analysis on an IS50 FTIR spectrometer (Nicolet, MA, Boston, USA) in the wavelength range of 4000–400 cm⁻¹. The scan was performed 16 times.

2.11. Triple-Helix Structural Analysis

The conformational structure of the IC-FWBP was determined by the Congo red method described in a previous report [8], with some modifications. Approximately 2 mL of the IC-FWBP solution (0.5 mg/mL) was mixed with 2 mL of Congo red (80 μM) with vigorous stirring, and then 1 M NaOH was added. The maximum absorbance wavelengths (λ_{max}) of the IC-FWBP+Congo red and Congo red were measured at different NaOH concentrations (0–0.5 M).

2.12. Scanning Electron Microscopy

IC-FWBP sample was coated with a gold thin layer using a JEC-3000FC Auto Fine Coater (JEOL, Tokyo, Japan) and then observed on a JSM-IT300LV scanning electron microscopy (SEM) system (JEOL, Tokyo, Japan) with an acceleration voltage of 10.0 kV and a magnification of 1000×.

2.13. Atomic Force Microscopy

Approximately 5 μL of the IC-FWBP solutions (10 μg/mL) was deposited on freshly lysed mica plates and dried at room temperature. The sample was observed on a MultiMode 8 atomic force microscopy (AFM) system equipped with a silicon Nanoprobes SPM tip (TESPA-V2, Bruker, Santa Barbara, CA, USA) in tapping mode.

2.14. Thermal Analysis

Thermogravimetric analysis (TGA) of the IC-FWBP was performed on a Q50 thermogravimetric analyzer [24]. Approximately 5 mg of the IC-FWBP sample was placed into an

aluminum crucible and heated from 30 °C to 600 °C at a heating rate of 10 °C/min under nitrogen flow.

Differential scanning calorimetry (DSC) of the IC-FWBP was analyzed using a DSC-60Plus system (Shimadzu Corporation, Kyoto, Japan). Accurately 3.2 mg of the IC-FWBP was subjected to DSC measurement, and the temperature was set from 30 °C to 250 °C at a heating rate of 10 °C/min. The onset temperature (T_o), denaturation peak temperature (T_p), endset temperature (T_e) and enthalpy change ($-\Delta H$) of IC-FWBP were determined.

3. Results and Discussion

3.1. Extraction and Purification of Polysaccharides from Fermented Wheat Bran

The crude polysaccharides were isolated from the solid-state fermented wheat bran by the IC strain, with a yield of 13.39%, whereas the yield was 5.60% when extracted from raw wheat bran. The crude polysaccharide extracts were further purified by a DEAE-52 cellulose column (Figure 1A). The IC-FWBP fraction was eluted with 0.1 M sodium chloride (NaCl), followed by dialysis and lyophilization. The yield of the IC-FWBP fraction was 2.88% (Table 1). The IC-FWBP contained a large amount of total sugar (91.63%), a small amount of uronic acid (9.67%) and protein (2.33%) (Table 1). Figure 1B shows a single peak of the IC-FWBP with an average M_w of 3.31×10^6 Da and PDI of 1.02.

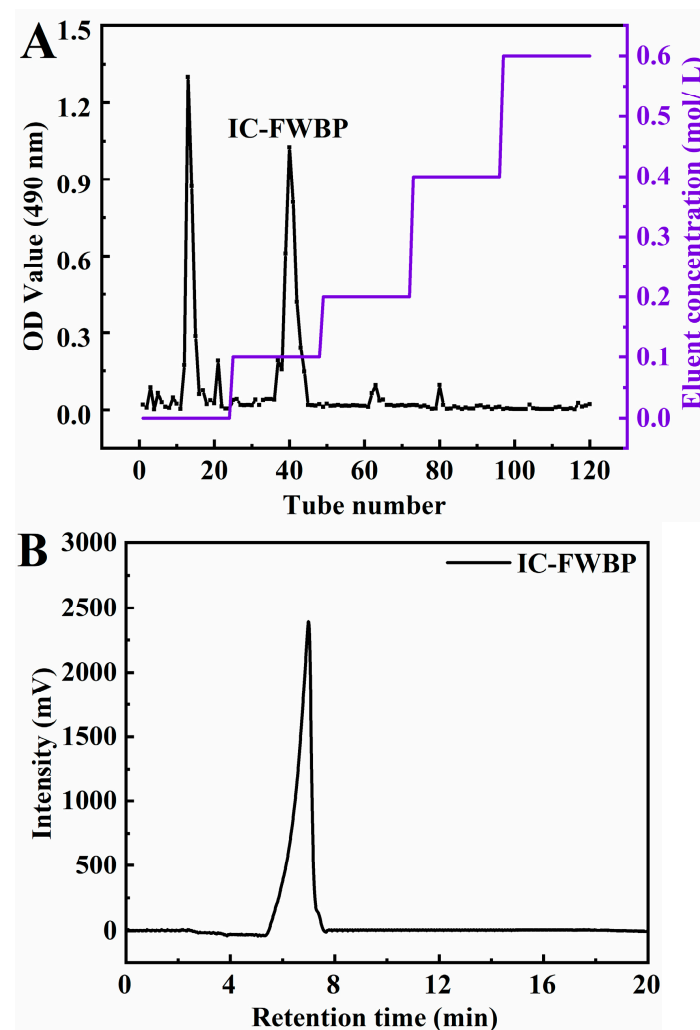


Figure 1. (A) Chromatography of the crude polysaccharides by DEAE-52 column; (B) HPLC profiles of IC-FWBP.

Table 1. Compositional, molecular, and structural features of the IC-FWBP.

Contents	IC-FWBP
M_n ($\times 10^6$ Da)	3.24
M_w ($\times 10^6$ Da)	3.31
M_w/M_n	1.02
Total sugar (%) ^a	91.63 \pm 0.98
Uronic acid (%) ^a	9.67 \pm 0.61
Protein (%) ^a	2.33 \pm 0.27
Mannose (%) ^b	41.33
Glucose (%) ^b	23.13
Galactose (%) ^b	35.54
Yield (%) ^a	2.88 \pm 0.12

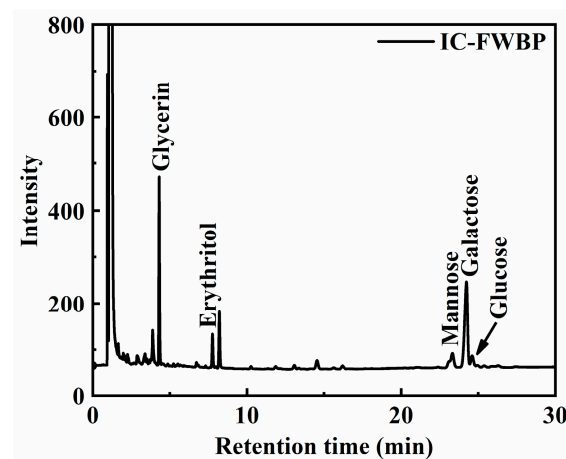
^a expressed as % of the sample dry matter; ^b expressed as mol. %.

3.2. Monosaccharide Composition Analysis

The IC-FWBP is a type of heteropolysaccharide, mainly comprised of mannose, glucose and galactose (Figure S1). As shown in Table 1, the IC-FWBP contained mannose (41.33%), glucose (23.13%), and galactose (35.54%). Similar compositions of the monosaccharides were found in the polysaccharide extracts from *Cordyceps cicadae* [13]. However, although the monosaccharide compositions of wheat bran polysaccharides varied with wheat species, sources, processing conditions, etc., they were mainly composed of glucose, galactose, xylose, and arabinose [8]. The results indicated that the soluble sugars in wheat bran, such as arabinoxylans (pentose), were converted to *Cordyceps cicadae* polysaccharides (hexose) with different structural features during solid-state fermentation of wheat bran by IC strains (Table S2).

3.3. Periodate Oxidation and Smith Degradation

The periodate oxidation result showed that the IC-FWBP consumed sodium periodate and released formic acid, suggesting the existence of (1 \rightarrow) or (1 \rightarrow 6)-linked glycosidic bonds. The consumption of sodium periodate was more than twice the amount of formic acid, indicating the existence of one or more (1 \rightarrow 2), (1 \rightarrow 4), or (1 \rightarrow 6)-linked glycosidic bonds [25]. The Smith degradation result of the IC-FWBP is shown in Figure 2. The presence of glycerol indicates the existence of (1 \rightarrow 2) or (1 \rightarrow 6)-linked glycosidic bonds [26]; erythritol, (1 \rightarrow 4) or (1 \rightarrow 4,6)-linked pyranosidic bonds or (1 \rightarrow 5) or (1 \rightarrow 5,6)-linked furanosidic bonds [27]; monosaccharides (mannose, galactose, and glucose) indicates (1 \rightarrow 3), (1 \rightarrow 3,6), (1 \rightarrow 2,3), (1 \rightarrow 3,4), (1 \rightarrow 2,4), (1 \rightarrow 2,3,4) or (1 \rightarrow 2,3,6)-linked glycosidic bonds [28]. Several glycosidic bonds were precisely confirmed by the methylation and NMR spectral analyses.

**Figure 2.** Gas chromatography of the Smith degradation of the IC-FWBP.

3.4. Methylation Analysis

The methylation analysis was performed to determine the glycosidic bond types of the IC-FWBP (Table 2). Five peaks were identified in the IC-FWBP: 2,3,4,6-Me₄-Glc, 3,4,6-Me₃-Man, 2,3-Me₂-Gal, 6-Me-Gal and 6-Me-Man, with molar ratios of 26.42:18.04:9.48:22.39:23.67. The methylation result was consistent with that of the monosaccharide composition analysis. It partially concluded that linkage types contained (1→)-linked glucose, (1→2)-linked mannose, (1→5,6)-linked galactose, (1→2,3,4)-linked galactose and (1→2,3,4)-linked mannose. These inferences were consistent with the results of the periodate oxidation and Smith degradation. *Cordyceps sinensis* polysaccharides are usually composed of glucose (Glc), mannose (Man) and galactose (Gal) in various mole ratios [29]. A backbone composed of mannose and a branched chain composed of galactose, mannose and glucose were found in the *Cordyceps sinensis* fungus UM01 [30].

Table 2. GC-MS data for methylated sugar moieties of the IC-FWBP.

Sample	Type of Linkage	Methylated Alditol Acetates	Major Mass Fragment (m/z)	Molar Ratio
IC-FWBP				
A	T-Glcf	2,3,4,6-Me ₄ -Glc	43;87;101;117;161;205	26.42
B	1,2-Manp	3,4,6-Me ₃ -Man	43;87;101;129;161;189	18.04
C	1,5,6-Galf	2,3-Me ₂ -Gal	43;85;101;117;127;161;201;261	9.48
D	1,2,3,4-Galp	6-Me-Gal	43;115;145;187;217;259;289	22.39
E	1,2,3,4-Manp	6-Me-Man	43;115;145;187;217;259;289	23.67

3.5. NMR Spectral Analysis

One-dimensional (1D) and two-dimensional (2D) NMR spectra containing ¹H, ¹³C, ¹H-¹H COSY, HSQC, and HMBC were allowed to determine the detailed structure information, including the monosaccharide, α -/ β -anomeric configurations, linkage types, and sequences [31]. In general, the α -anomeric protons are in the δ 4.8–5.8 ppm region, and the β -anomeric protons are in the δ 4.2–4.8 ppm region within the area [32]. The anomeric NMR signals for the protons of polysaccharides are typically observed in the chemical shift range of 3.0–5.8 ppm [33], while the chemical shifts around 3.4–4.2 ppm are generally considered to be signals associated with protons present at C2–C6 [34]. The NMR data on glycosidic linkages of the IC-FWBP are assigned and listed in Table 3. Notably, the chemical shifts at 106.06 and 107.77 ppm were attributed to C-1 of β -furanose units because of extremely low field shifts [35]. Consistent with the above information on monosaccharides, β -D-Glcf(1→, →2)- α -D-Manp(1→, →5,6)- β -D-Galf(1→, →2,3,4)- α -D-Galp(1→, and →2,3,4)- β -D-Manp(1→) were identified from the NMR data of IC-FWBP. In the ¹H NMR spectra (Figure 3A), the anomeric proton signals at δ 5.17, 5.08, 5.05, 4.87 and 4.62 ppm were assigned as A, B, C, D and E. The signals at δ 5.08 and 4.87 (residues B and D) were ascribed to the α -linked residues, while the others (residues A, C and E) contained β -anomeric protons. In the ¹³C NMR spectrum (Figure 3B), five anomeric C signals were also identified at δ 97.88, 99.77, 100.72, 106.27 and 107.76 ppm. The results were consistent with the methylation analysis of IC-FWBP.

In the ¹H-¹H COSY spectrum (Figure 3C), the α -anomeric proton of residue A was located at δ 5.17 ppm. δ 5.17/ δ 4.18 was attributed to the H1/H2 correlation of the T- β -D-Glcf residue. Thus, the proton correlations of the IC-FWBP were noticed in Table 3. The ¹H-¹³C HSQC spectrum (Figure 3D and Figure S2) shows five pairs of ¹H and ¹³C signals of anomeric H/C, which are caused by five different glycosidic bonds. The proton correlations of IC-FWBP were also noted in Table 3. According to the chemical shifts of protons and relevant HSQC correlations, the signals δ 5.17/106.27 (AH1/C1), δ 5.08/97.88 (BH1/C1), δ 5.05/107.76 (CH1/C1), δ 4.87/100.72 (DH1/C1) and δ 4.62/99.77 (EH1/C1) were detected, suggesting five sugar residues existed in the IC-FWBP. In agreement with the methylation result as well as ¹H, ¹³C, and COSY analyses, residues A–E were assigned as T- β -D-Glcf, 1→2- α -D-Manp, 1→5,6- β -D-Galf, 1→2,3,4- α -D-Galp and 1→2,3,4- β -D-Manp, respectively.

Table 3. Assignments of ^{13}C NMR and ^1H NMR chemical shifts of the IC-FWBP.

Sample	Sugar Residue	Chemical Shift (ppm)					
		C1/H1	C2/H2	C3/H3	C4/H4	C5/H5	C6/H6
IC-FWBP							
A	$\beta\text{-D-Glcf}(1\rightarrow$	106.27/5.17	86.59/4.18	72.50/3.64	69.75/3.38	70.72/3.67	60.99/3.70
B	$\rightarrow 2)\text{-}\alpha\text{-D-Manp}(1\rightarrow$	97.88/5.08	69.10/3.66	70.56/3.81	76.22/3.39	72.67/3.75	60.84/3.91
C	$\rightarrow 5,6)\text{-}\beta\text{-D-Galf}(1\rightarrow$	107.76/5.05	80.92/4.13	72.37/3.29	75.85/3.45	76.23/3.77	66.70/3.89
D	$\rightarrow 2,3,4)\text{-}\alpha\text{-D-Galp}(1\rightarrow$	100.72/4.87	70.23/4.14	80.44/3.69	71.82/3.53	69.69/3.37	60.65/3.76
E	$\rightarrow 2,3,4)\text{-}\beta\text{-D-Manp}(1\rightarrow$	99.77/4.62	83.03/3.98	72.39/3.63	75.69/3.50	73.75/3.22	60.86/3.72

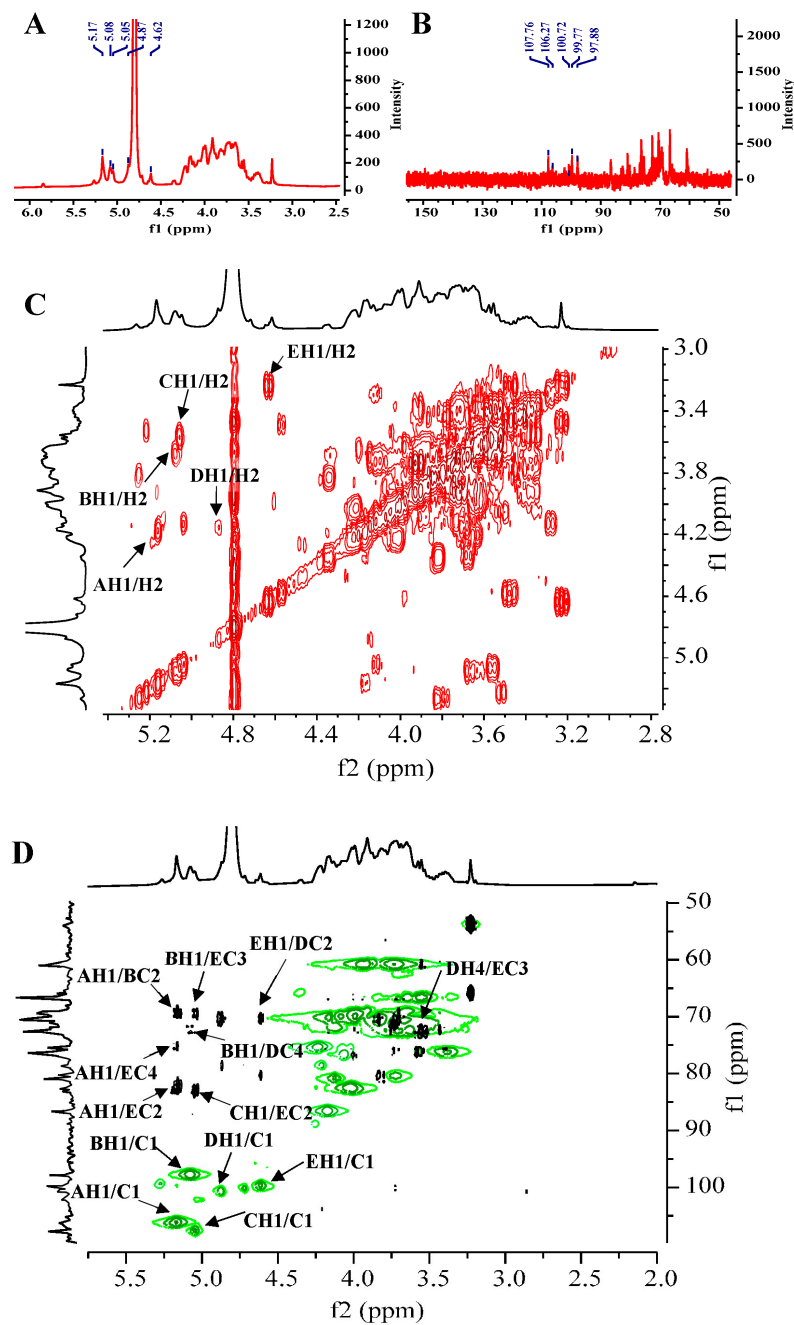


Figure 3. 1D and 2D NMR spectra of the IC-FWBP (A–D). (A) ^1H NMR spectra; (B) ^{13}C NMR spectra; (C) $^1\text{H}\text{-}^1\text{H}$ COSY spectra; $^1\text{H}\text{-}^{13}\text{C}$ HSQC spectra (in green color) and $^1\text{H}\text{-}^{13}\text{C}$ HMBC spectra (in black color) were overlapped in (D).

The ^1H - ^{13}C HMBC spectrum (Figure 3D and Figure S3) showed the correlations of five sugar residues in the IC-FWBP as follows: AH1/BC2 at δ 5.17/69.10, BH1/EC3 at δ 5.08/72.39, CH1/EC2 at δ 5.05/83.03, EH1/DC2 at δ 4.62/70.23, DH4/EC3 at δ 3.53/72.39, AH1/EC4 at δ 5.17/75.69, AH1/EC2 at δ 5.17/83.03 and BH1/DC4 at δ 5.08/71.82. The structure of the IC-FWBP contained a backbone made up of 1 \rightarrow 2- α -D-Manp, 1 \rightarrow 2,3,4- α -D-Galp and 1 \rightarrow 2,3,4- β -D-Manp. The branching substitute was composed of T- β -D-Glcf and 1 \rightarrow 5,6- β -D-Galf. Summed up, the inferred structure of the IC-FWBP is illustrated in Figure 4.

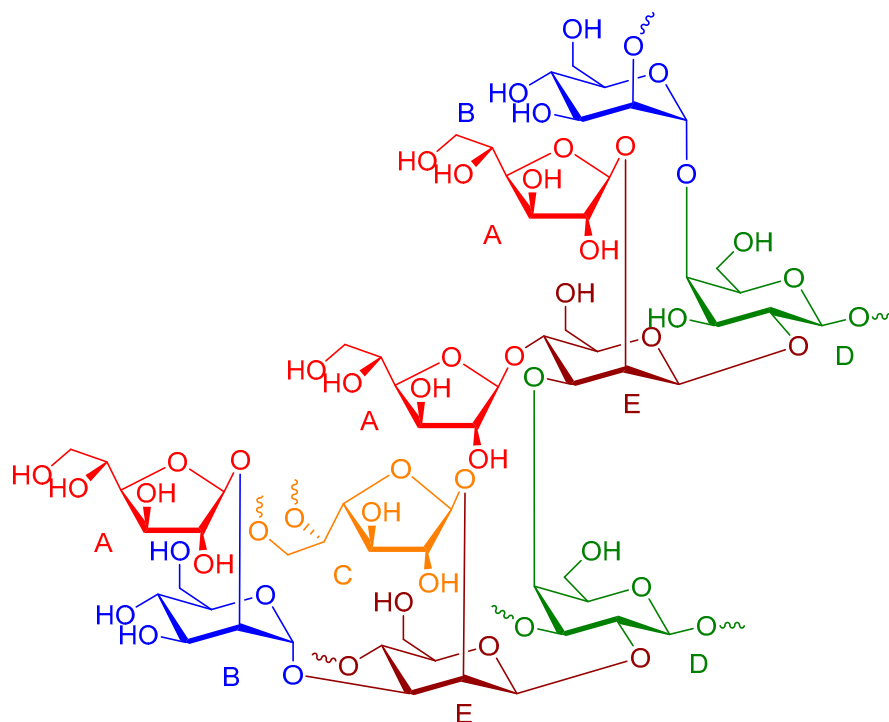


Figure 4. Inferred structure of the IC-FWBP.

3.6. FTIR Spectral Analysis

The functional groups of the IC-FWBP were analyzed by FTIR spectroscopy. As shown in Figure 5A, the strong and broad absorption peak at 3428 cm^{-1} corresponded to the OH stretching vibrations, and the weak absorption peak at around 2930 cm^{-1} was attributed to the C-H stretching vibrations of alkyl groups in the IC-FWBP, which were two typically characteristic absorptions of polysaccharide. The absorption peaks at 1640 cm^{-1} and 1413 cm^{-1} of the IC-FWBP were ascribed to the C=O and C=C stretching vibrations, respectively [36]. The IC-FWBP presented stronger absorption at 1640 cm^{-1} , confirming the existence of the uronic acid in the IC-FWBP, which was consistent with the result of the chemical composition analysis in Table 1.

3.7. Triple-Helix Structural Analysis

The triple-helix conformations of the IC-FWBP were identified by the Congo red method. Congo red is an acidic dye, and it can form a complex with the polysaccharide with a triple-helix structure under weak alkaline conditions, resulting in a red shift of the maximum ultraviolet absorption wavelength (λ_{max}) [37]. Figure 5B shows that compared with Congo red, the λ_{max} of the complexes (IC-FWBP+Congo red) is red shifted, indicating the existence of a triple helical structure [38]. However, when the NaOH concentration exceeded 0.25 M, the λ_{max} of IC-FWBP+Congo red first decreased and then tended to be stable, which might be due to the disintegration of parts of triple helical structures into irregular helical structures [39].

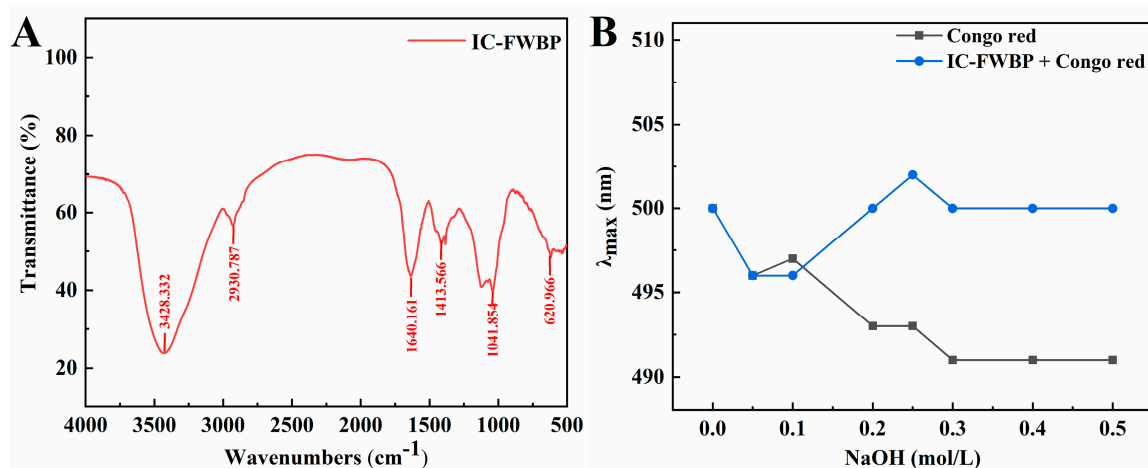


Figure 5. (A) FTIR spectral analysis and the triple-helix conformation analysis (B) of the IC-FWBP.

3.8. Morphological Observation

Figure 6 shows the morphological observations of IC-FWBP. The SEM images (Figure 6A) exhibited that the surface of the IC-FWBP was composed of rod-like and spherical particles. Figure 6B presents the surface of the IC-FWBP fractions by AFM. A large number of spherical clusters of different sizes were obviously shown in AFM images, indicating intermolecular aggregation between polysaccharide chains. These morphological features may be due to the existence of hydrogen bonds in intramolecular and intermolecular interactions, which promote the aggregation of polysaccharide molecules [40].

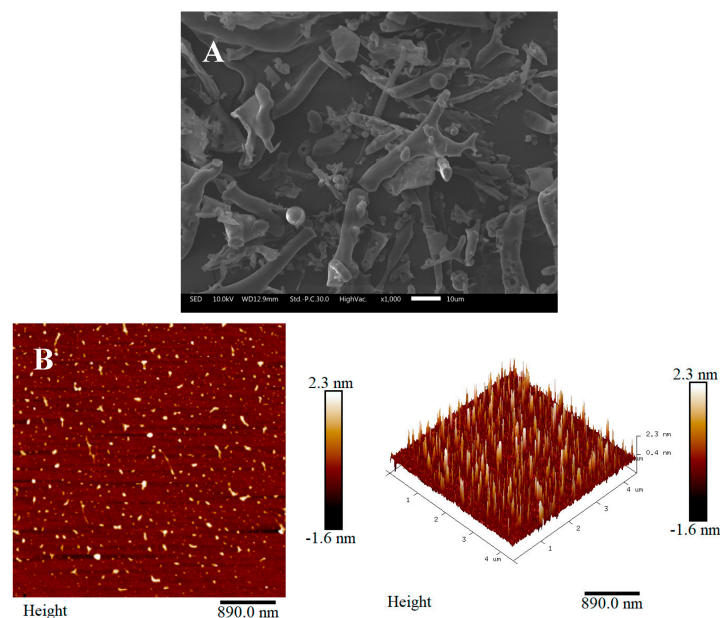


Figure 6. (A) Scanning electron micrographs of the IC-FWBP; (B) atomic force microscopy images of the IC-FWBP.

3.9. Thermal Analysis

The thermal stability of the IC-FWBP was examined by TGA and DSC (Figure 7 and Table 4). Due to the loss of water, the initial weight loss occurred with the degradation temperature ranging from 28 °C to 150 °C. The degradation peak temperatures of the IC-FWBP were 275.40 °C. Furthermore, the DSC analysis result of IC-FWBP was shown in

Table 4 and Figure S4. Two endothermic peaks appeared in the IC-FWBP during heating. The peak temperatures for IC-FWBP were 88.06 °C and 206.79 °C, respectively.

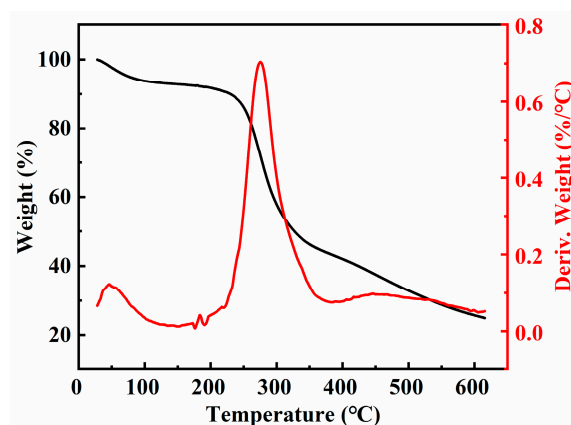


Figure 7. Thermogravimetry and derivative thermogravimetry curves of IC-FWBP.

Table 4. The DSC results of IC-FWBP.

Sample	T_o (°C)	T_p (°C)	T_e (°C)	$-\Delta H$ (J/g)
IC-FWBP	25.54	88.06	126.34	848.60
	150.41	206.79	261.37	915.81

4. Conclusions

In this study, the polysaccharide fraction of IC-FWBP was first isolated from solid-state fermented wheat bran by *Isaria cicadae* Miq. The structural analysis results indicated that the IC-FWBP had an average M_w of 3.31×10^6 Da, and was mainly comprised of glucose, galactose and mannose, with a uronic acid content of 9.67%. The IC-FWBP contained glycosidic linkages of T- β -D-Glcf, 1 \rightarrow 2- α -D-Manp, 1 \rightarrow 5,6- β -D-Galf, 1 \rightarrow 2,3,4- α -D-Galp and 1 \rightarrow 2,3,4- β -D-Manp, with a triple-helix conformation. In addition, the morphological observation showed that the IC-FWBP was composed of rod-like and spherical particles. This study provides a theoretical basis for further research on the functional properties of IC solid-state fermented wheat bran polysaccharide and the structure-activity relationship.

Supplementary Materials: The following supporting information can be downloaded at: <https://www.mdpi.com/article/10.3390/fermentation9030309/s1>, Figure S1: Gas chromatography of standard monosaccharides (A) and FWBP (B); Figure S2: 1H-13C HSQC spectrum of the IC-FWBP; Figure S3: 1H-13C HMBC spectrum of the IC-FWBP; Figure S4: DSC analysis curve of FWBP; Table S1: The chemical composition of the wheat bran powder; Table S2: Compositional features of the raw wheat bran polysaccharides (RWBPs).

Author Contributions: Conceptualization, R.L. (Rui Liu); methodology, N.L.; software, R.L. (Ruixin Liu); validation, N.L.; formal analysis, N.L.; investigation, N.L.; resources, M.L., B.G. and M.Z.; data curation, N.L.; writing—original draft preparation, R.L. (Rui Liu) and R.L. (Ruixin Liu); writing—review and editing, Z.Z. and X.Y.; visualization, N.L.; supervision, R.L. (Rui Liu); project administration, R.L. (Rui Liu); funding acquisition, R.L. (Rui Liu) and B.G. All authors have read and agreed to the published version of the manuscript.

Funding: The research was supported by the project of the National Natural Science Foundation of China (No. 31972012; No. 32111530082), the project of the Key Laboratory of Agro-Products Processing and Storage, the Key Laboratory of Agro-products Quality and Safety Control in Storage and Transport Process, the Ministry of Agriculture and Rural Affairs, P. R. China (No. S2022KFKT-01) and the project of the Tianjin Education Commission (No. 2018KJ089).

Institutional Review Board Statement: Not applicable.

Informed Consent Statement: Not applicable.

Data Availability Statement: Not applicable.

Conflicts of Interest: The authors declare that they have no known competing financial interests or personal relationships that could have appeared to influence the work reported in this paper.

References

1. Xu, M.J.; Yan, T.X.; Gong, G.W.; Wu, B.; He, B.S.; Du, Y.Y.; Xiao, F.; Jia, Y. Purification, structural characterization, and cognitive improvement activity of a polysaccharides from *Schisandra chinensis*. *Int. J. Biol. Macromol.* **2020**, *163*, 497–507. [[CrossRef](#)] [[PubMed](#)]
2. Olawuyi, I.F.; Kim, S.R.; Hahn, D.; Lee, W.Y. Influences of combined enzyme-ultrasonic extraction on the physicochemical characteristics and properties of okra polysaccharides. *Food Hydrocolloid.* **2020**, *100*, 105396. [[CrossRef](#)]
3. Muthusamy, S.; Udayakumar, G.P.; Narala, V.R. Recent advances in the extraction and characterization of seed polysaccharides, and their bioactivities: A review. *Bioact. Carbohydr. Diet. Fibre.* **2021**, *26*, 100276. [[CrossRef](#)]
4. Chen, G.J.; Yuan, Q.X.; Saeeduddin, M.; Ou, S.Y.; Zeng, X.X.; Ye, H. Recent advances in tea polysaccharides: Extraction, purification, physicochemical characterization and bioactivities. *Carbohydr. Polym.* **2016**, *153*, 663–678. [[CrossRef](#)] [[PubMed](#)]
5. Ge, J.C.; Zha, X.Q.; Nie, C.Y.; Yu, N.J.; Li, Q.M.; Peng, D.Y.; Duan, J.; Pan, L.H.; Luo, J.P. Polysaccharides from *Dendrobium huoshanense* stems alleviates lung inflammation in cigarette smoke-induced mice. *Carbohydr. Polym.* **2018**, *189*, 289–295. [[CrossRef](#)]
6. Su, Y.; Li, L. Structural characterization and antioxidant activity of polysaccharide from four auriculariales. *Carbohydr. Polym.* **2020**, *229*, 115407. [[CrossRef](#)]
7. Ferreira, S.S.; Passos, C.P.; Madureira, P.; Vilanova, M.; Coimbra, M.A. Structure–function relationships of immunostimulatory polysaccharides: A review. *Carbohydr. Polym.* **2015**, *132*, 378–396. [[CrossRef](#)]
8. Lv, Q.Q.; Cao, J.J.; Liu, R.; Chen, H.Q. Structural characterization, alpha-amylase and alpha-glucosidase inhibitory activities of polysaccharides from wheat bran. *Food Chem.* **2021**, *341*, 128218. [[CrossRef](#)]
9. Tian, X.L.; Wang, Z.; Yang, S.K.; Wang, X.X.; Li, L.; Sun, B.H.; Ma, S.; Zheng, S.Q. Microstructure observation of multilayers separated from wheat bran. *GOST* **2021**, *4*, 165–173. [[CrossRef](#)]
10. Hussain, A.; Bose, S.; Wang, J.-H.; Yadav, M.K.; Mahajan, G.B.; Kim, H. Fermentation, a feasible strategy for enhancing bioactivity of herbal medicines. *Food Res. Int.* **2016**, *81*, 1–16. [[CrossRef](#)]
11. Chen, Q.Y.; Wang, R.F.; Wang, Y.; An, X.P.; Liu, N.; Song, M.; Yang, Y.P.; Yin, N.; Qi, J.W. Characterization and antioxidant activity of wheat bran polysaccharides modified by *Saccharomyces cerevisiae* and *Bacillus subtilis* fermentation. *J. Cereal Sci.* **2021**, *97*, 103157. [[CrossRef](#)]
12. Lu, X.J.; Jing, Y.; Li, Y.Y.; Zhang, N.S.; Cao, Y.G. *Eurotium cristatum* produced β -hydroxy acid metabolite of monacolin K and improved bioactive compound contents as well as functional properties in fermented wheat bran. *LWT-Food Sci. Technol.* **2022**, *158*, 113088. [[CrossRef](#)]
13. Xu, Z.C.; Yan, X.T.; Song, Z.Y.; Li, W.; Zhao, W.B.; Ma, H.H.; Du, J.L.; Li, S.J.; Zhang, D.Y. Two heteropolysaccharides from *Isaria cicadae* Miquel differ in composition and potentially immunomodulatory activity. *Int. J. Biol. Macromol.* **2018**, *117*, 610–616. [[CrossRef](#)] [[PubMed](#)]
14. Wang, H.; Yang, Z.; Chen, K.; Yu, R.L.; Xu, L.; Lv, G.H. *Isaria cicadae* Miquel prevents intestinal fibrosis by activating transforming growth factor- β 1 signaling to regulate the balance between matrix metalloproteinases and tissue inhibitors of metalloproteinase 1 in mice with Crohn’s disease. *J. Funct. Foods* **2022**, *88*, 104875. [[CrossRef](#)]
15. Xu, Z.C.; Lin, R.Y.; Hou, X.H.; Wu, J.; Zhao, W.B.; Ma, H.H.; Fan, Z.Y.; Li, S.J.; Zhu, Y.; Zhang, D.Y. Immunomodulatory mechanism of a purified polysaccharide isolated from *Isaria cicadae* Miquel on RAW264.7 cells via activating TLR4-MAPK-NF-kappaB signaling pathway. *Int. J. Biol. Macromol.* **2020**, *164*, 4329–4338. [[CrossRef](#)]
16. Qin, D.; Han, S.; Liu, M.; Guo, T.; Hu, Z.; Zhou, Y.; Luo, F. Polysaccharides from *Phellinus linteus*: A systematic review of their extractions, purifications, structures and functions. *Int. J. Biol. Macromol.* **2023**, *230*, 123163. [[CrossRef](#)]
17. Dubois, M.; Gilles, K.A.; Hamilton, J.K.; Rebers, P.A.; Smith, F. Colorimetric method for determination of sugars and related substances. *Anal. Chem.* **1956**, *28*, 350–356. [[CrossRef](#)]
18. Chu, E.P.; Tavares, A.R.; Kanashiro, S.; Giampaoli, P.; Yokota, E.S. Effects of auxins on soluble carbohydrates, starch and soluble protein content in *Aechmea blanchetiana* (Bromeliaceae) cultured in vitro. *Sci. Hortic-Amsterdam.* **2010**, *125*, 451–455. [[CrossRef](#)]
19. Taylor, K.A.C.C. A Colorimetric Method for the Quantitation of Galacturonic Acid. *Appl. Biochem. Biotech.* **1993**, *43*, 51–54. [[CrossRef](#)]
20. Jiang, J.Y.; Kong, F.S.; Li, N.S.; Zhang, D.Z.; Yan, C.Y.; Lv, H.C. Purification, structural characterization and in vitro antioxidant activity of a novel polysaccharide from Boshuzhi. *Carbohydr. Polym.* **2016**, *147*, 365–371. [[CrossRef](#)]
21. Shi, Y.Y.; Xiong, Q.P.; Wang, X.L.; Li, X.; Yu, C.H.; Wu, J.; Yi, J.; Zhao, X.J.; Xu, Y.; Cui, H. Characterization of a novel purified polysaccharide from the flesh of *Cipangopaludina chinensis*. *Carbohydr. Polym.* **2016**, *136*, 875–883. [[CrossRef](#)] [[PubMed](#)]
22. Li, G.Q.; Chen, P.F.; Zhao, Y.T.; Zeng, Q.H.; Ou, S.Y.; Zhang, Y.H.; Wang, P.C.; Chen, N.H.; Ou, J.Y. Isolation, structural characterization and anti-oxidant activity of a novel polysaccharide from garlic bolt. *Carbohydr. Polym.* **2021**, *267*, 118194. [[CrossRef](#)] [[PubMed](#)]

23. You, Y.; Song, H.R.; Wang, L.L.; Peng, H.R.; Sun, Y.J.; Ai, C.Q.; Wen, C.R.; Zhu, B.W.; Song, S. Structural characterization and SARS-CoV-2 inhibitory activity of a sulfated polysaccharide from *Caulerpa lentillifera*. *Carbohydr. Polym.* **2022**, *280*, 119006. [[CrossRef](#)] [[PubMed](#)]
24. Hou, Q.D.; Li, W.Z.; Ju, M.T.; Liu, L.; Chen, Y.; Yang, Q.; Wang, J.Y. Separation of polysaccharides from rice husk and wheat bran using solvent system consisting of BMIMOAc and DMI. *Carbohydr. Polym.* **2015**, *133*, 517–523. [[CrossRef](#)]
25. Chen, J.C.; Li, L.; Zhou, X.; Li, B.; Zhang, X.; Hui, R. Structural characterization and alpha-glucosidase inhibitory activity of polysaccharides extracted from Chinese traditional medicine Huidouba. *Int. J. Biol. Macromol.* **2018**, *117*, 815–819. [[CrossRef](#)]
26. Zhang, H.; Zou, P.; Zhao, H.T.; Qiu, J.Q.; Regenstein, J.M.; Yang, X. Isolation, purification, structure and antioxidant activity of polysaccharide from pinecones of *Pinus koraiensis*. *Carbohydr. Polym.* **2021**, *251*, 117078. [[CrossRef](#)]
27. Zhong, R.F.; Yang, J.J.; Geng, J.H.; Chen, J. Structural characteristics, anti-proliferative and immunomodulatory activities of a purified polysaccharide from *Lactarius volemus* Fr. *Int. J. Biol. Macromol.* **2021**, *192*, 967–977. [[CrossRef](#)]
28. Xu, J.; Chen, Z.Y.; Liu, P.H.; Wei, Y.; Zhang, M.; Huang, X.D.; Peng, L.L.; Wei, X.L. Structural characterization of a pure polysaccharide from *Bletilla striata* tubers and its protective effect against H₂O₂-induced injury fibroblast cells. *Int. J. Biol. Macromol.* **2021**, *193*, 2281–2289. [[CrossRef](#)]
29. Yan, J.K.; Wang, W.Q.; Wu, J.Y. Recent advances in *Cordyceps sinensis* polysaccharides: Mycelial fermentation, isolation, structure, and bioactivities: A review. *J. Funct. Foods*. **2014**, *6*, 33–47. [[CrossRef](#)]
30. Cheong, K.-L.; Meng, L.-Z.; Chen, X.-Q.; Wang, L.-Y.; Wu, D.-T.; Zhao, J.; Li, S.-P. Structural elucidation, chain conformation and immuno-modulatory activity of glucogalactomannan from cultured *Cordyceps sinensis* fungus UM01. *J. Funct. Foods* **2016**, *25*, 174–185. [[CrossRef](#)]
31. Rodriguez Sanchez, R.A.; Matulewicz, M.C.; Ciancia, M. NMR spectroscopy for structural elucidation of sulfated polysaccharides from red seaweeds. *Int. J. Biol. Macromol.* **2021**, *199*, 386–400. [[CrossRef](#)] [[PubMed](#)]
32. Qian, K.Y.; Cui, S.W.; Nikiforuk, J.; Goff, H.D. Structural elucidation of rhamnogalacturonans from flaxseed hulls. *Carbohydr. Res.* **2012**, *362*, 47–55. [[CrossRef](#)] [[PubMed](#)]
33. Yu, Z.Y.; Liu, L.; Xu, Y.Q.; Wang, L.B.; Teng, X.; Li, X.G.; Dai, J. Characterization and biological activities of a novel polysaccharide isolated from raspberry (*Rubus idaeus* L.) fruits. *Carbohydr. Polym.* **2015**, *132*, 180–186. [[CrossRef](#)]
34. Wang, L.B.; Liu, F.C.; Wang, A.; Yu, Z.Y.; Xu, Y.Q.; Yang, Y. Purification, characterization and bioactivity determination of a novel polysaccharide from pumpkin (*Cucurbita moschata*) seeds. *Food Hydrocolloid.* **2017**, *66*, 357–364. [[CrossRef](#)]
35. Chen, Y.; Mao, W.; Wang, J.; Zhu, W.; Zhao, C.; Li, N.; Wang, C.; Yan, M.; Guo, T.; Liu, X. Preparation and structural elucidation of a glucomannogalactan from marine fungus *Penicillium commune*. *Carbohydr. Polym.* **2013**, *97*, 293–299. [[CrossRef](#)]
36. Xiang, A.N.; Li, W.T.; Zhao, Y.N.; Ju, H.M.; Xu, S.; Zhao, S.Y.; Yue, T.L.; Yuan, Y.H. Purification, characterization and antioxidant activity of selenium-containing polysaccharides from pennycress (*Thlaspi arvense* L.). *Carbohydr. Res.* **2022**, *512*, 108498. [[CrossRef](#)]
37. Tan, M.H.; Zhao, Q.S.; Zhao, B. Physicochemical properties, structural characterization and biological activities of polysaccharides from quinoa (*Chenopodium quinoa* Willd.) seeds. *Int. J. Biol. Macromol.* **2021**, *193*, 1635–1644. [[CrossRef](#)]
38. Zhang, X.L.; Zhang, X.J.; Gu, S.S.; Pan, L.C.; Sun, H.Q.; Gong, E.L.; Zhu, Z.Y.; Wen, T.C.; Daba, G.M.; Elkhateeb, W.A. Structure analysis and antioxidant activity of polysaccharide-iron (III) from *Cordyceps militaris* mycelia. *Int. J. Biol. Macromol.* **2021**, *178*, 170–179. [[CrossRef](#)]
39. Hui, H.P.; Li, X.Z.; Jin, H.; Yang, X.Y.; Xin, A.Y.; Zhao, R.M.; Qin, B. Structural characterization, antioxidant and antibacterial activities of two heteropolysaccharides purified from the bulbs of *Lilium davidii* var. unicolor Cotton. *Int. J. Biol. Macromol.* **2019**, *133*, 306–315. [[CrossRef](#)]
40. Kong, L.S.; Yu, L.; Feng, T.; Yin, X.J.; Liu, T.J.; Dong, L. Physicochemical characterization of the polysaccharide from *Bletilla striata*: Effect of drying method. *Carbohydr. Polym.* **2015**, *125*, 1–8. [[CrossRef](#)]

Disclaimer/Publisher’s Note: The statements, opinions and data contained in all publications are solely those of the individual author(s) and contributor(s) and not of MDPI and/or the editor(s). MDPI and/or the editor(s) disclaim responsibility for any injury to people or property resulting from any ideas, methods, instructions or products referred to in the content.